JOURNAL OF SOLID STATE CHEMISTRY 79, 157–168 (1989)

Superconducting properties and Structural Study of $Bi_{2-x}Pb_xSr_2Ca_{1-x}Y_xCu_2O_8$ ($0 \leq x \leq 1$)

R. RETOUX, V. CAIGNAERT, J. PROVOST, C. MICHEL, M. HERVIEU, AND B. RAVEAU

Laboratoire de Cristallographie et Sciences des Matériaux, ISMRa, Boulevard du Maréchal Juin, F-14032 Caen Cédex, France

Received December 1, 1988

A solid solution has been prepared by coupled substitution of lead for bismuth and yttrium for calcium in the $Bi_2Sr_2CaCu_2O_8$ cuprates. Pure phases $Bi_{2-x}Pb_xSr_2Ca_{1-x}Y_xCu_2O_8$ were obtained from $x = 0$ to $x = 1$. The superconducting properties of the samples vary with x: T_c remains close to 85 K up to $x = 0.5$ and then decreases drastically. The variation of the cell parameters has been studied: the oxides possess an orthorhombic cell with $a = 5.385$ Å, $b = 5.424$ Å, and $c = 30.316$ Å, with a space group *Pnam* for $x = 1$. The electron diffraction patterns are complex; several types of satellites have been observed and were correlated with distortions, twins, and short-range order phenomena. Local variations of the Bi/Pb ratio most likely occur and could be responsible for the change in T_c.

Following the observation of superconductivity at 22 K in the Bi–Sr–Cu–O system (*1*) and intensive investigation of bismuth cuprates led to the discovery of superconductors with higher critical temperature. In addition to the 22 K superconductor $Bi_2Sr_2CuO_6$, two other cuprates are now known: $Bi_2Sr_2CaCu_2O_8$, called "2212" (*2–7*), and $Bi_2Sr_2Ca_2Cu_3O_{10}$, called "2223" (*8–10*), which superconduct below 80 and 110 K, respectively. The structure of these three phases may be described as an intergrowth of triple-distorted rock-salt-type layers and multiple oxygen-deficient perovskite layers according to the general formula $[(BiO)_2SrO][SrCa_{m-1}Cu_mO_{2m+1}]$ with $m = 1, 2, 3$ for the "2201", "2212", and "2223" superconductors, respectively. Among these compounds, the latter is the most difficult to obtain as a pure phase since it cannot be synthesized from the oxides and carbonates in appropriate stoichiometric proportions. Endo *et al.* (*9*) have demonstrated that an excess of calcium and copper oxides, and addition of PbO, are essential to obtain the "2223" phase without impurities. In recent papers (*11, 12*) we showed that it is possible to replace copper by iron in the "2212" and "2223" phases, leading to the oxides $Bi_2Sr_2CaFe_2O_9$, $Bi_2Sr_3Fe_2O_9$, and $Bi_2Sr_4Fe_3O_{12}$, which are not superconductors. Substitutions of yttrium and lanthanides for calcium in $Bi_2Sr_2CaCu_2O_8$ were extensively studied by Tarascon *et al.* (*13*). These authors found that superconductivity disappeared for approximately 75% of substitution whereas T_c remained approximately constant up to a 25% substitution level. The mechanism of superconductivity in these oxides is far from be-

0022-4596/89 $3.00

ing understood. However, the replacement of divalent calcium by trivalent yttrium or lanthanide, which involves an excess of oxygen with respect to the stoichiometric formula can explain the disappearance of superconductivity in the substituted compounds; it indeed involves a decrease of the mean valence of copper or a lack of the bidimensionality of the structure, if excess oxygen is located at the lanthanide level (or yttrium).

We report here on the coupled substitution of lead for bismuth and yttrium for calcium in the "2212" cuprate, i.e., on the oxide $Bi_{2-x}Pb_xSr_2Ca_{1-x}Y_xCu_2O_8$.

Experimental

The $Bi_{2-x}Pb_xSr_2Ca_{1-x}Y_xCu_2O_8$ series were prepared by reacting Bi_2O_3, CuO, PbO, Y_2O_3, $SrCO_3$ and $CaCO_3$ in stoichiometric proportions. Powders were mixed and ground, then pressed into pellets which were placed in alumina boats and heated in air, with the following thermal procedure: a heating rate of 50°C hr^{-1} up to 800°C; a dwelling time of 36 hr at this temperture, then 6 days at 865°C; lastly, cooling to room temperature at a cooling rate of 50°C hr^{-1}.

Samples were analyzed by powder X-ray diffraction and the diffractograms recorded on a Philips goniometer using Cu$K\alpha$ radiation.

Electron diffraction studies were performed on a JEOL 120 CX microscope, fitted with a eucentric goniometer (±60°).

The superconducting properties were studied by resistance measurements, using the classical four-probe method, and by flux expulsion, using a SQUID magnetometer.

Results and Discussion

The X-ray analysis shows that the simultaneous replacement of calcium by yttrium and of a part of bismuth by lead is possible, and that a continuous solid solution exists from $Bi_2Sr_2CaCu_2O_8$ to $BiPbSr_2YCu_2O_8$. All the reflections of the X-ray powder diffraction patterns can be indexed in an orthorhombic cell with parameters close to those observed for $Bi_2Sr_2CaCu_2O_8$ (a = 5.404 Å, b = 5.406 Å, c = 30.78 Å from our measurements). The cell parameters are plotted in Fig. 1 as a function of the substitution x. From this figure, it can be seen that the introduction of lead and yttrium into the "2212" superconductor leads to a sharp decrease of the c parameter and to a

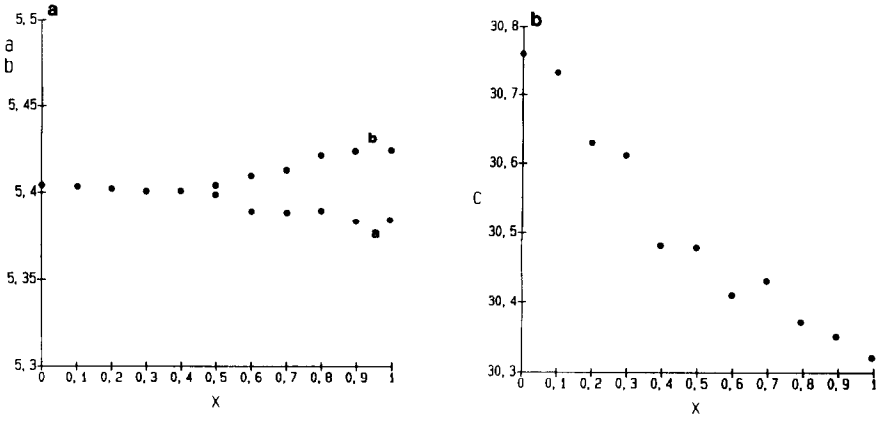

FIG. 1. (a–b) Evolution of the cell parameters (in Å) as a function of x for the oxides $Bi_{2-x}Pb_xSr_2Ca_{1-x}Y_xCu_2O_8$.

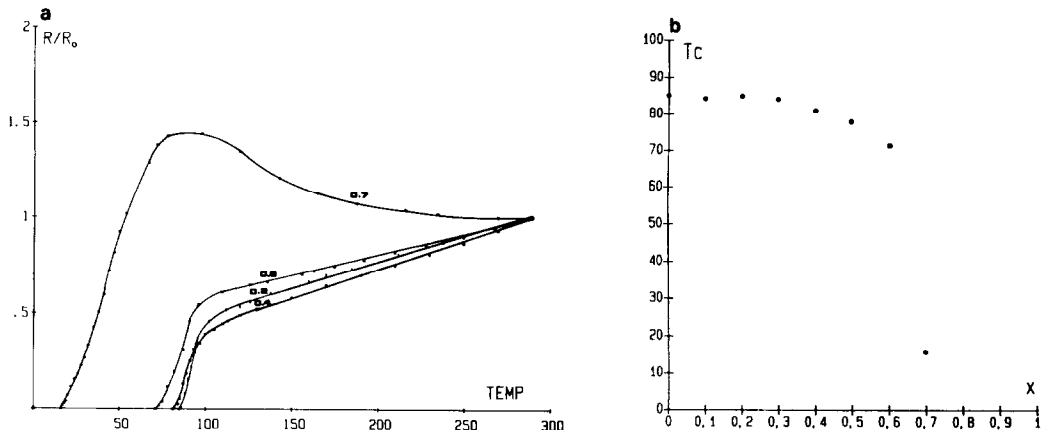

FIG. 2. Superconducting properties of the series $Bi_{2-x}Pb_xSr_2Ca_{1-x}Y_xCu_2O_8$: (a) resistivity measurements for some x values, (b) variation of T_c at $R = 0$ as a function of x.

large increase of the orthorhombic distortion for high x values ($x > 0.5$), as shown, for example, for the limiting compound $BiPbSr_2YCu_2O_8$ ($a = 5.385$ Å, $b = 5.424$ Å, $c = 30.316$ Å).

The superconducting properties of the different oxides of the series $Bi_{2-x}Pb_xSr_2Ca_{1-x}Y_xCu_2O_8$ have been studied. Some of the resistivity measurements are plotted in Fig. 2a. Up to $x \sim 0.5$, $\rho_{300\,K}$ remains approximately constant and exhibits metallic behavior. For higher x values, ρ increases with increasing x, and semiconducting behavior is observed. For example, for $x = 0.8$, the resistivity at room temperature is about 20 times larger than for $x = 0.5$. No resistance transition is measured for $x > 0.7$. T_c at $\rho = 0$ remains close to 85 K up to $x = 0.5$, and then decreases drastically (Fig. 2b), whereas T at the top of the resistivity downturn seems to have a constant value ($T \sim 90$ K) all over the series where the superconducting transition is observed. The magnetization measurements allow diamagnetism to be observed up to $x = 0.8$ (less than 1% of diamagnetism at 4.2 K for this composition). The magnetic behavior of the limit composition $BiPbSr_2YCu_2O_8$, which exhibits antiferromagnetic order below 20 K, is quite similar to that observed by Fukushima *et al.* (*14*) for $Bi_2Sr_2YCu_2O_8$. The change in T_c offset is to be compared with the results obtained by Tarascon *et al.* (*13*) on the members of the series $Bi_2Sr_2Ca_{1-x}Ln_xCu_2O_{8+y}$ (Ln = Tm, Eu, Er, Ho). In these latter compounds, T_c remains constant up to $x \sim 0.25$, then decreases toward zero for $x = 0.75$. Correspondingly, the mean oxidation state for copper decreases from 2.15 ($x = 0$) to 2.07 ($x = 1$).

From the electron diffraction investigation of $BiPbSr_2YCu_2O_8$ samples, it appears that the limiting composition exhibits a mica-like morphology, similar to that previously mentioned for $Bi_2Sr_2CuO_6$ (*1*), $Bi_2Sr_2CaCu_2O_8$ (*7, 15–18*), and $Bi_{1.8}Pb_{0.2}Sr_2CaCu_2O_8$ (*19*). An example is shown in Fig. 3, where the splitting of the crystal is clearly visible. Two important points emerge from this study:

—The highly complex features observed especially in [001] ED patterns which will be further discussed,

—the reciprocal space analysis performed on several microcrystals shows that the space group is no longer *Amaa*, as observed in $Bi_2Sr_2CaCu_2O_8$ (*3–7*). The condi-

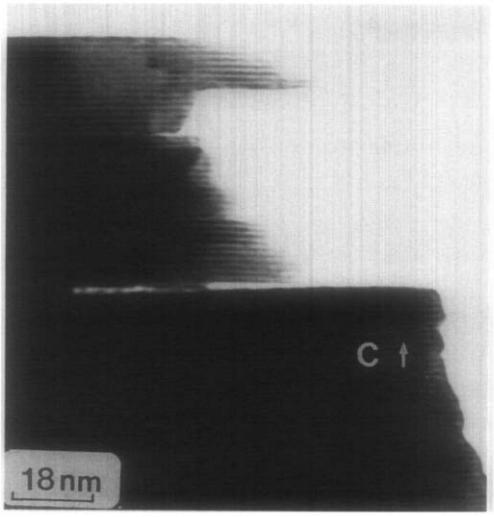

FIG. 3. [001] image of $BiPbSr_2YCu_2O_8$: mica-like morphology. Note the splitting of the crystal in thin slices.

tions of systematic reflections are: hkl, no cond, $0kl$, $k + l = 2n$, $h0l$, $h = 2n$ involving the space group *Pnam*. Three ED patterns, [100], [010], and [110], are shown in Fig. 4. The $h0l$ reflections with $l = 2n + 1$ are clearly visible; $00l$ reflections with $l = 2n + 1$ arise from double diffraction phenomena.

A detailed observation of the X-ray diffraction diagram showed that no extra lines resulted from this change in symmetry. Moreover, all the reflections—except one observed for $2\theta = 16.60°$ whose relative intensity is less than 1/100 of the largest peak—can be indexed in an F space group.

In order to check the isomorphism of both limiting compositions, $Bi_2Sr_2CaCu_2O_8$ and $BiPbSr_2YCu_2O_8$, a powder structure study of the latter compound was undertaken.

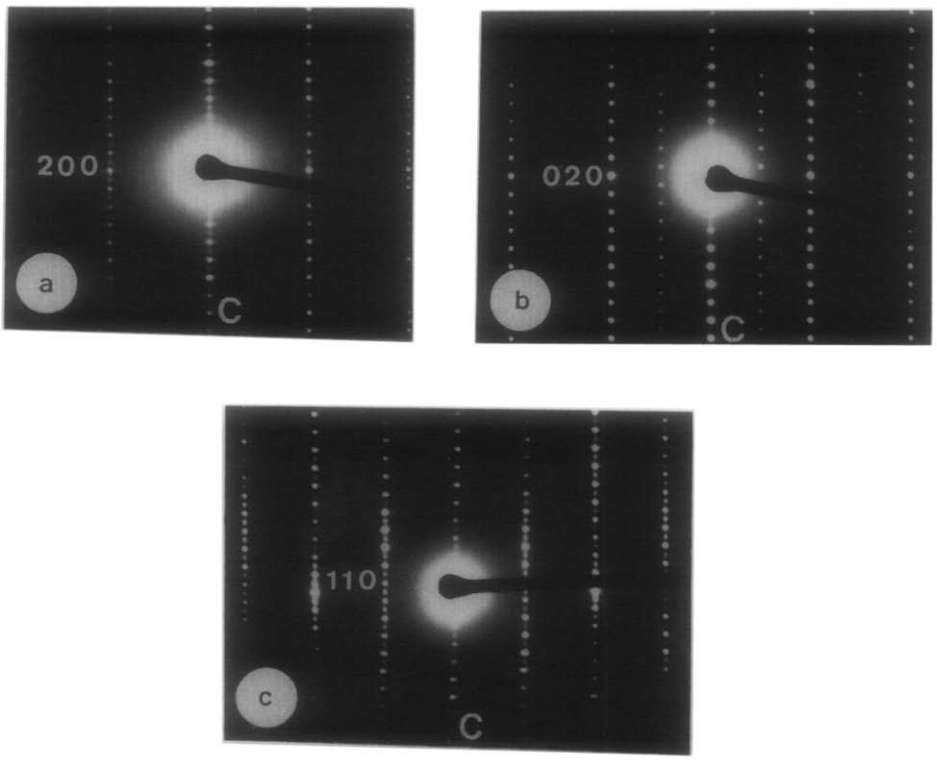

FIG. 4. Electron diffraction patterns: (a) [010], (b) [100], (c) [110], registered for $BiPbSr_2YCu_2O_8$.

Because of the weak set of reflections, and taking into account the above considerations, this study was carried out in the space group *Fmmm* which corresponds to a smaller number of possible diffraction lines with respect to *Amaa*. Calculations were performed with the first 23 visible intensities, i.e., 56 *hkl*. In order to limit the number of variables, and because of the small value of the scattering factor of oxygen relative to those of the metallic elements, the isotropic thermal factor of the oxygen atoms was arbitrarily fixed at 1.0 Å^2. The nature of the Bi(Pb)–O layers was assumed to be of rock-salt-type. To take into account the mica-like character of the oxide, a preferential orientation parameter G along [001] was included in the calculations. After successive refinements of the positional parameters of all elements, of the preferential orientation parameter, and of the thermal factor of the metallic constituents, the discrepancy factor, $R = \Sigma|I_o - I_c|/\Sigma I_o$, was decreased to 0.069 for the values presented in Table I. Interatomic metal–oxygen distances are shown in Table II.

These results confirm the possibility of a partial substitution of lead for bismuth, coupled with a complete substitution of yttrium for calcium in $Bi_2Sr_2CaCu_2O_8$ (Fig. 5) without any drastic change of the structure, despite the observed drastic decrease of the c parameter with increasing x, in this series; this parameter, for $x = 1$, remains greater than that observed for $Bi_2Sr_2YCu_2O_{8+\delta}$ (*13*, *14*). Such a decrease of the c parameter has already been observed in the thallium cuprate $TlBa_2YCu_2O_7$ (*20*) relative to the "1212" thallium superconductor $TlBa_2CaCu_2O_7$.

The above structural determination cannot be considered accurate because of the small number of data and the large errors concerning the oxygen positions. However, the following features can be considered significant:

(i) The relatively small B value obtained for the Bi(Pb) atoms shows that, contrary to the case of $Bi_2Sr_2CaCu_2O_8$, these atoms are not displaced from the "ideal" positions. The distance along **c** between two ad-

TABLE I

STRUCTURAL DATA FOR $BiPbSr_2YCu_2O_8$ IN SPACE GROUP *Fmmm* (R = 0, 069; G = 0.4)

Cation	Site	x	y	z	B (Å^2)
Bi, Pb	8i	0.0	0.0	0.2018 (6)	1.2
Sr	8i	0.0	0.0	0.6147 (9)	2.3
Y	4b	0.0	0.0	0.5	1.2
Cu	8i	0.0	0.0	0.0554 (13)	1.3
O(1)	16j	1/4	1/4	0.049 (2)	1.0
O(2)	8i	0.0	0.0	0.686 (4)	1.0
O(3)	8i	0.0	0.0	0.133 (5)	1.0

TABLE II

INTERATOMIC DISTANCES (Å)

Bi, Pb–O(2)	2.73 ×2	Y–O(1)	2.40 ×8
Bi, Pb–O(2)	2.75 ×2		
Bi, Pb–O(2)	3.40 ×1	Cu–O(1)	1.92 ×4
Bi, Pb–O(2)	2.07 ×1	Cu–O(3)	2.37 ×1
Sr–O(1)	2.78 ×4		
Sr–O(2)	2.16 ×2		
Sr–O(3)	2.77 ×2		
Sr–O(3)	2.75 ×2		

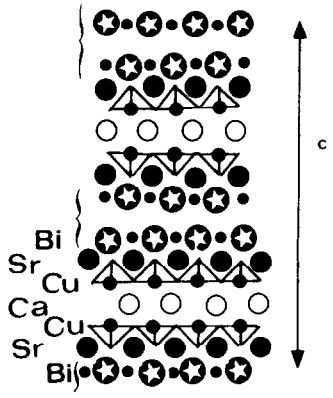

FIG. 5. Structure of the superconductor $Bi_2Sr_2CaCu_2O_8$.

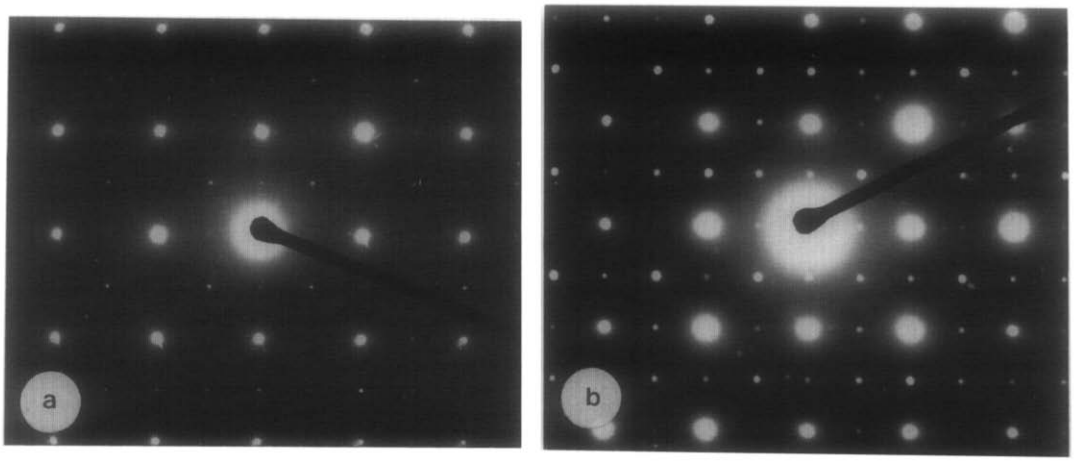

FIG. 6. Variation of the intensity of the extra spots of the *P* space group with respect to the *F* space group.

jacent Bi(Pb) layers (2.9 Å), is slightly smaller than in the "2212" superconductor ($d \sim 3.1$ Å), but remains large enough to explain the mica-like character of this oxide. Such behavior, and especially the values of those distances, can be attributed to the stereoactivity of the $6s^2$ lone pairs of both cations Bi(III) and Pb(II) and confirm their respective oxidation states.

(ii) The distance between the oxygen atoms of two successive $[CuO_2]_\infty$ layers (d = 2.91 Å) is shorter than that observed in $Bi_2Sr_2CaCu_2O_8$ (d = 3.01 Å), leading to Y–O(1) distances smaller than the Ca–O distances in the superconducting oxide. Such a phenomenon, which tends to lead to cubic symmetry in the YO_8 polyhedron, as compared to the CaO_8 polyhedron has already been observed in $TlBa_2YCu_2O_7$ (*20*). At the same time the O–O distance along **c** becomes smaller, the Cu–Cu distance becomes larger: d_{Cu-Cu} = 3.36 Å, compared to 3.27 Å in the pure bismuth cuprate, leading to copper displaced by about 0.2 Å toward the center of the CuO_5 pyramid. This distance remains too short to permit insertion of oxygen atoms at the level of yttrium. Thus, it seems that the three phenomena—the decrease of the O–O distance, the increase of the Cu–Cu distances between two successive adjacent layers, and the decrease of the tetragonal distortion of the YO_8 or CaO_8 group—are closely related to each other and involve a decrease of T_c, leading to the disappearance of superconductivity.

As already mentioned, the [001] ED patterns exhibit various and complex features. the most striking are:

(i) The intensities of the $hk0$ reflections relative to the basic spots of the *F* subcell vary from one crystal to another. Very faint spots are observed in Fig. 6a, whereas many strong spots are present in Fig. 6b; but, whatever their relative intensities may be, they are always observed. Some of these ED patterns show a splitting of the reflections (Fig. 7) characteristic of twinning; the twin plane is [010], i.e., $[110]_p$ plane of the perovskite subcell.

(ii) Contrary to the situation in $Bi_2Sr_2CaCu_2O_8$, crystals which exhibit satellites along the *A* axis are rare. Two examples are shown in Figs. 8a and 8b: in both cases, they occur in incommensurate positions.

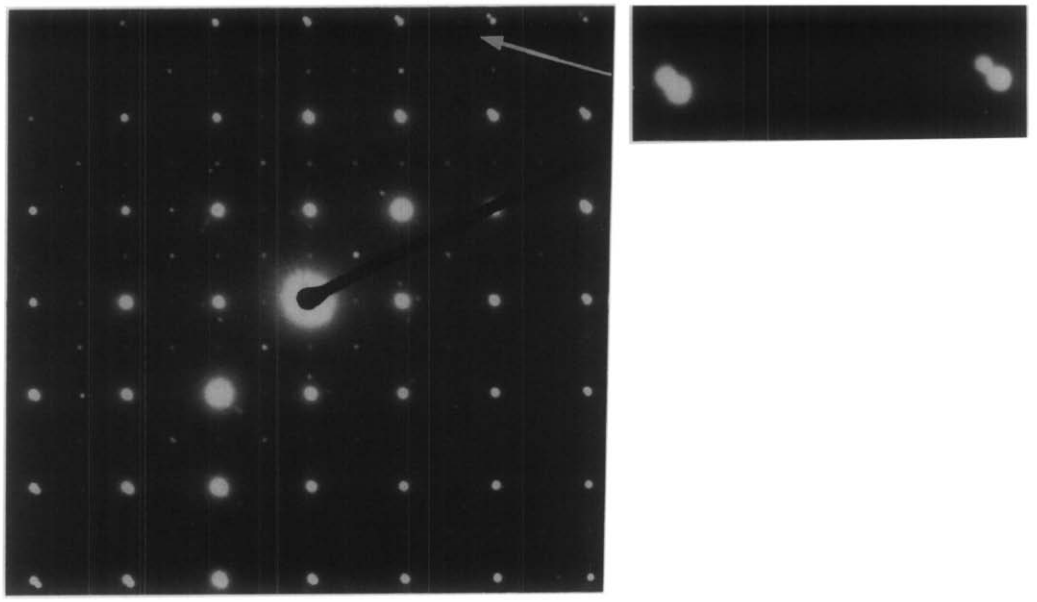

FIG. 7. Splitting of the reflections characteristic of the twinned crystals. [001] Electron diffraction pattern.

This feature is similar to that observed in $Bi_2Sr_2CaCu_2O_8$ (*7, 15–18*) but in the present case, the satellites are always weak; we observed generally only the satellites of first order. The q value close to 5.25 is, however, different from that of pure Bi phases. Note that they are observed as well in patterns where the relative intensity of the $hk0$ extra reflections of the P group is weak, as in patterns where this relative intensity is

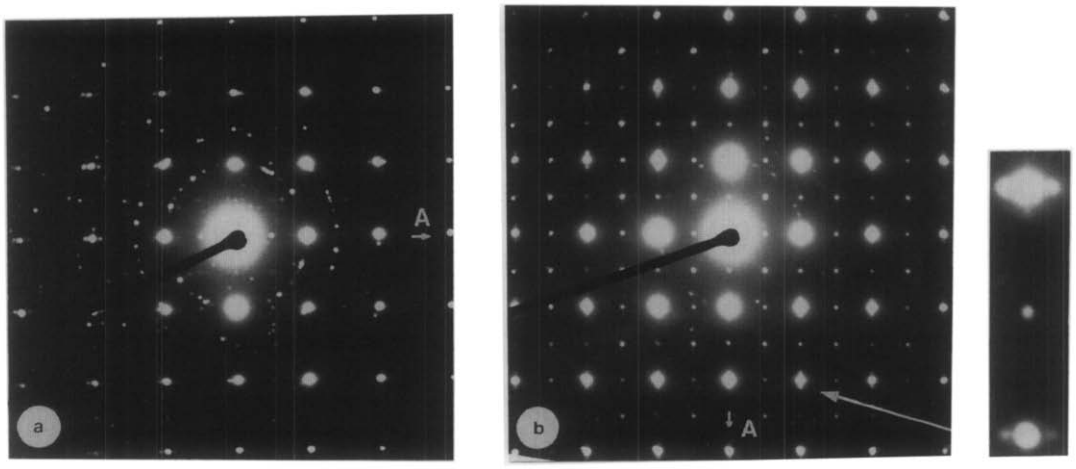

FIG. 8. (a) Examples of satellites along the A direction. The q value is close to 5.25. This type of crystal is rare. (b) The satellites arise only near the strong reflections (F group). This feature can be correlated with the existence of different regions in the crystal.

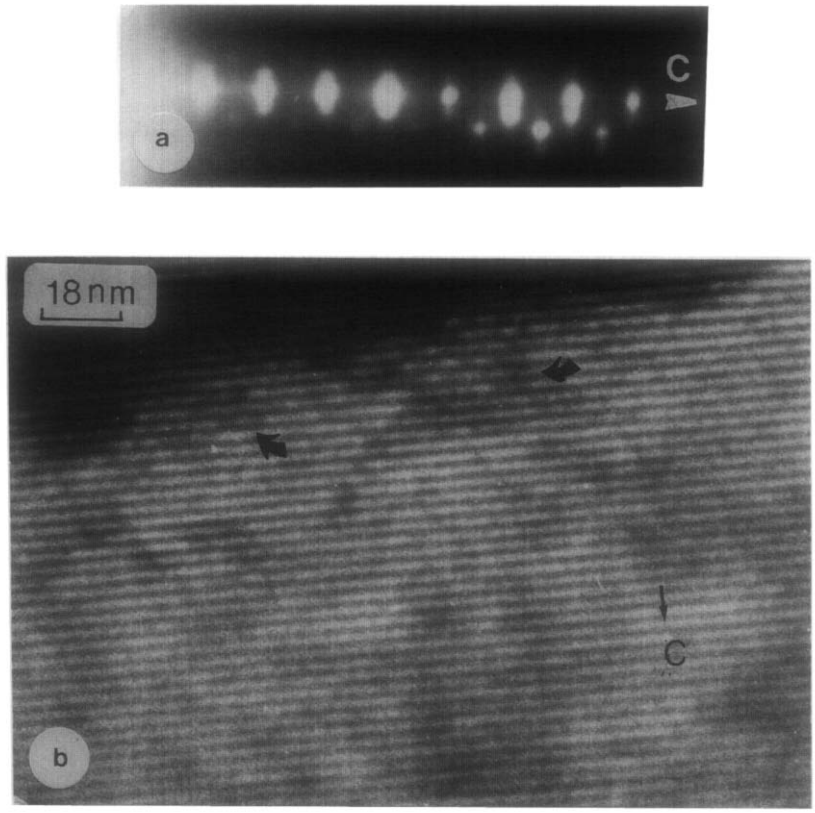

FIG. 9. (a) Weak satellites can be observed in slightly tilted (001) planes. (b) Corresponding images showing the existence of local modulations (indicated by arrows).

strong (Figs. 8a and 8b, respectively). However, in the latter case the extra spots have no satellites: this can be interpreted as a superposition of both types of patterns. Indeed, weak satellites can be observed in slightly tilted *h0l* planes (Fig. 9a). The corresponding bright field image shows the existence of modulations similar to those observed in the pure Bi oxides (*15–18, 21–24*), but only in small regions of the crystals. This suggests that the rare crystals (or crystal areas) which exhibit this phenomenon would correspond to a ratio Bi/Pb greater than that of the nominal composition.

(iii) Other types of incommensurate satellites are shown in Figs. 10a and 10b. They arise from the superposition of disoriented lamellae. Such features were previously reported in $Bi_{1.8}Pb_{0.2}Sr_2CaCu_2O_8$ (*19*) and $Tl_{0.5}Pb_{0.5}Sr_2CaCu_2O_7$ (*20*). Both components are clearly visible in Fig. 10a, where the subcell reflections appear as the strongest spots; the weakest spots correspond either to the extra reflections of the *P* space group or to multiple diffraction phenomena, as previously reported (*25*). The angles ϕ between the axis of the different components are quite constant from one crystal to the other, as is also observed for $Tl_{0.5}Pb_{0.5}Sr_2CaCu_2O_7$. In the $BiPbSr_2YCu_2O_8$ crystals, ϕ is close to 99.9°; the ϕ value, which is reproducible, is significant and points to a structural feature as the origin of the misorientation.

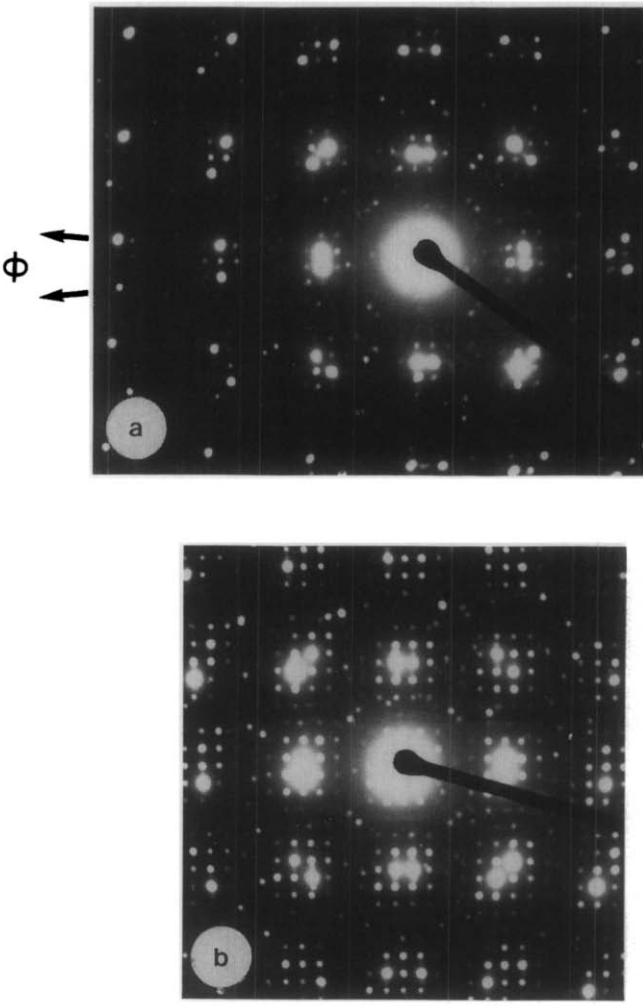

FIG. 10. Examples of satellites arising from misoriented areas in the crystals.

(iv) Still other types of satellites are observed. It should be noted that these different features can occur in the same crystal. A spectacular example is shown in Fig. 11 where five types of ED patterns are observed in different regions of the same crystal:

—satellites in incommensurate positions (q = 6.25) set up along a direction roughly parallel to [210], i.e. $[310]_p$ of the perovskite subcell; a schematic drawing is shown next to the micrograph (Fig. 11a);

—misoriented areas with ϕ = 99.9° (Fig. 11b);

—satellites which arise along 110 (i.e., $[100]_p$ of the perovskite subcell) with q = 3.65 (Fig. 11c);

—the above satellites, which have disappeared, but have streaks remaining along the [110] direction (Fig. 11d);

—multisplitting of the spots and modulations with first-order satellites as shown in the enlargement; they are indicative of small variations of parameters, distortions, and microtwins (Fig. 11e).

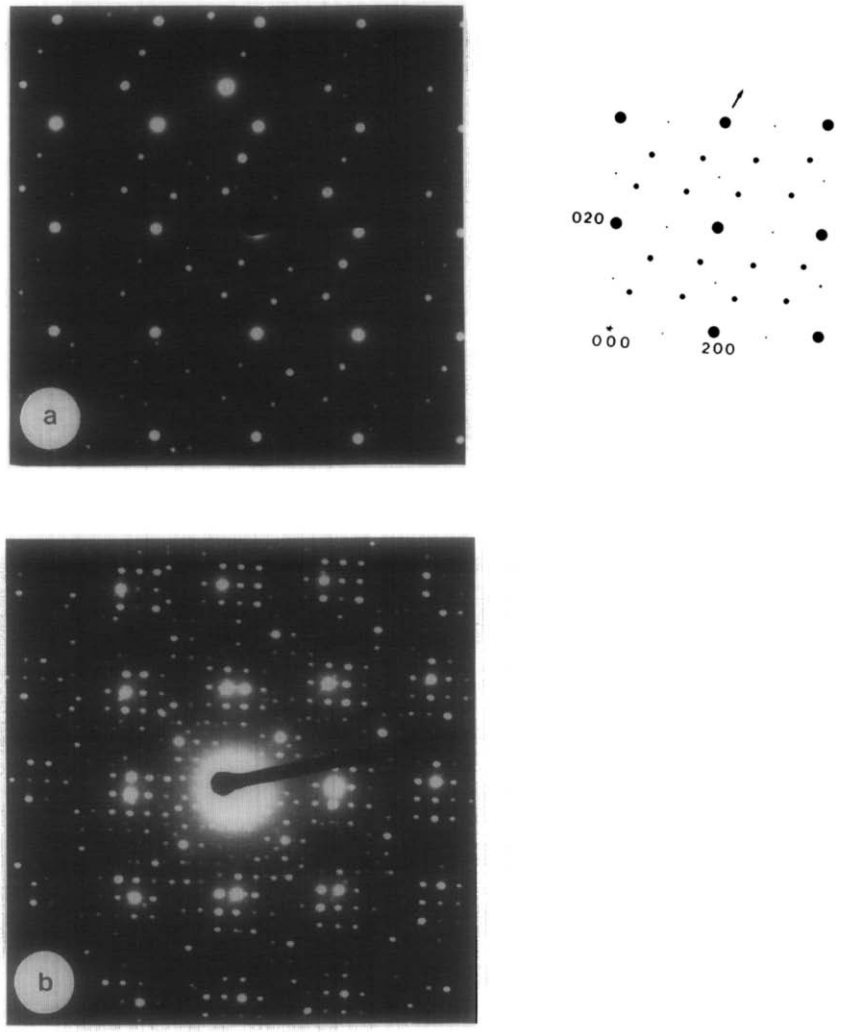

FIG. 11. [001] Electron diffraction patterns observed in different areas of one $BiPbSr_2YCu_2O_8$ crystal: (a) satellites set up along a direction roughly parallel to [210], (b) satellites arising from multiple diffraction phenomena in two misoriented areas (ϕ = 99.9°), (c) satellites along [110] direction, (d) satellites have disappeared but streaks remain along the [100] direction, (e) multisplitting of the *hk*0 reflections arising from small variations of parameters and microtwinning.

In conclusion, these results show clearly that bismuth can be replaced by lead over a wide homogeneity range, in agreement with the stereoactivity of the $6s^2$ lone pair of both cations Pb(II) and Bi(III). The disappearance of the systematical satellite spots along *A* observed for the substituted compound indicates once again that the bismuth bilayers are involved in the modulation. The introduction of lead involves new complex phenomena, in agreement with those previously reported for $Tl_{0.5}Pb_{0.5}Sr_2CaCu_2O_7$ (*25*). A local variation of the composition, i.e., of the Bi/Pb ratio appears most

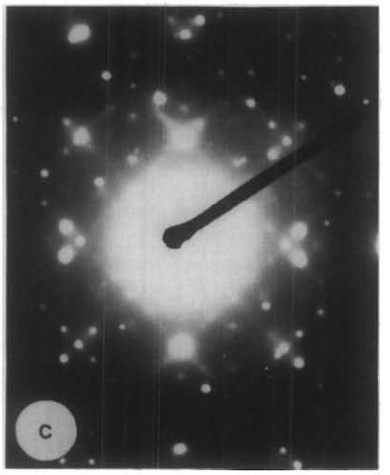

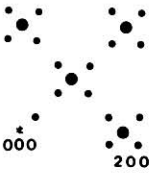

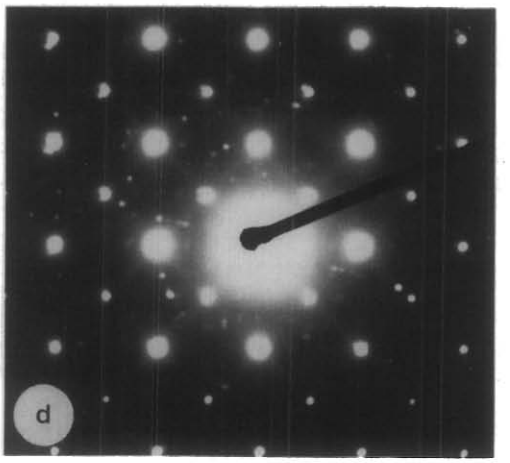

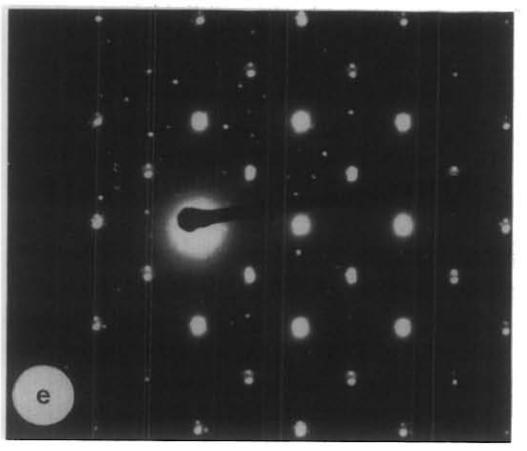

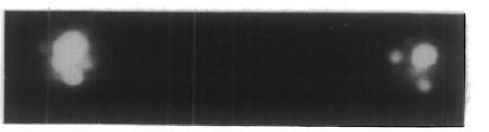

FIG. 11—*Continued.*

likely and could be responsible for the variations in T_c. An HREM investigation of this system is in progress.

References

1. C. MICHEL, M. HERVIEU, M. M. BOREL, A. GRANDIN, F. DESLANDES, J. PROVOST, AND B. RAVEAU, *Z. Phys. B* **68,** 421 (1987).
2. H. MAEDA, Y. TANAKA, M. FUKUTOMI, AND T. ASANO, *Japan. J. Appl. Phys.* **27,** L209 and L548 (1988).
3. M. A. SUBRAMANIAN, C. C. TORARDI, J. C. CALABRESE, J. GOPALAKRISHNAN, K. J. MORISSEY, T. R. ASKEW, R. B. FLIPPEN, V. CHOWDHRY, AND A. W. SLEIGHT, *Science* **239,** 1015 (1988).
4. J. M. TARASCON, Y. LE PAGE, P. BARBOUX, B. G. BAGLEY, L. H. GREENE, W. R. MCKINNON, G. W. HULL, M. GIROUD, AND D. M. HWANG, *Phys. Rev. B* **37,** 9382 (1988).
5. M. G. VON SCHNERING, L. WALZ, M. SCHWARTZ, W. BEKER, M. HARTWEG, T. POPP, B. HETTICH, P. MÜLLER, AND G. KAMPT, *Angew Chem.* **27,** 574 (1988).
6. C. POLITIS, *Appl. Phys. A* **45,** 261 (1988).
7. M. HERVIEU, C. MICHEL, B. DOMENGÈS, Y. LALIGANT, A. LEBAIL, G. FEREY, AND B. RAVEAU, *Mod. Phys. Lett. B* **2,** 491 (1988).
8. J. M. TARASCON, W. R. MCKINNON, P. BARBOUX, D. M. HWANG, B. G. BAGLEY, L. H. GREENE, G. HULL, Y. LE PAGE, N. STOFFEL, AND M. GIROUD, *Phys. Rev. B* **38,** 8885 (1988).
9. U. ENDO, S. KOYAMA, AND T. KAWAI, *Japan. J. Appl. Phys.* **27,** L1476 (1988).
10. M. MIZUMO, H. ENDO, J. TSUCHIYA, N. KIJIMA, A. SUMIYAMA, AND Y. OGURI, *Japan. J. Appl. Phys.* **27,** L1225 (1988).
11. M. HERVIEU, C. MICHEL, N. NGUYEN, R. RETOUX, AND B. RAVEAU, *J. Eur. Solid State Inorg. Chem.*, in press.
12. R. RETOUX, C. MICHEL, M. HERVIEU, N. NGUYEN, AND B. RAVEAU, *Solid State Commun.*, in press.
13. J. M. TARASCON, P. BARBOUX, G. W. HULL, R. RAMESH, L. H. GREENE, M. GIROUD, M. S. HEDGE, AND W. R. MCKINNON, *Phys. Rev. B,* in press.
14. N. FUKUSHIMA, H. NIU, AND K. ANDO, *Japan. J. Appl. Phys.* **28,** L1432 (1988).
15. M. HERVIEU, B. DOMENGÈS, C. MICHEL, AND B. RAVEAU, *Mod. Phys. Lett. B* **2,** 835 (1988).
16. G. VAN TENDELOO, H. W. ZANDBERGEN, J. VAN LANDUYT, AND S. AMELYNCKX, *Phys. C,* in press.
17. H. W. ZANDBERGEN, P. GRON, G. VAN TENDELOO, J. VAN LANDUYT, AND S. AMELYNCKX, *Solid State Commun.*, in press.
18. E. A. HEWAT, M. DUPUY, P. BORDET, C. CHAILLOUT, J. L. HODEAU, AND M. MAREZIO, *Nature (London)* **333,** 53 (1988).
19. J. L. HODEAU, P. BORDET, J. J. CAPPONI, C. CHAILLOUT, J. CHENEVAS, M. GODINHO, A. W. HEWAT, E. A. HEWAT, H. RENEVIER, A. M. SPIESER, P. STROBEL, J. L. THOLENCE, AND M. MAREZIO, *in* "Proceedings, First AS Pacific Conference on H T_c S, Singapore, June 27, 1988."
20. C. MARTIN, D. BOURGAULT, C. MICHEL, M. HERVIEU, AND B. RAVEAU, *Mod. Phys. Lett. B* **3,** 93 (1989).
21. F. KAKAYAMO-MUROMACHI, Y. UCHIOTO, A. ONO, F. IZUMI, AND M. ONODA, *Japan. J. Appl. Phys.* **27,** L365 (1988).
22. T. KIJIMA, J. TANAKA, Y. BANDO, M. ONODA, AND F. IZUMI, *Japan. J. Appl. Phys.* **27,** L369 (1988).
23. M. HERVIEU, C. MICHEL, AND B. RAVEAU, *J. Less-Common Met.*, in press.
24. P. L. GAI AND P. DAY, *Phys. C,* in press.
25. C. MARTIN, J. PROVOST, D. BOURGAULT, B. DOMENGÈS, C. MICHEL, M. HERVIEU, AND B. RAVEAU, *Phys. C,* in press.